STUDIA UBB CHEMIA, LXX, 2, 2025 (p. 163-178)
(RECOMMENDED CITATION)
DOI:10.24193/subbchem.2025.2.11

APPLICATION OF BANANA BASED AGRO-WASTE AS A PRECURSOR OF HETEROGENEOUS CATALYST FOR BIODIESEL PRODUCTION

Santhosh VISWANATHAN[a*], Siva PERIYASAMY[b], Senthilkumar KANDASAMY[c]

ABSTRACT. In the recent decades, the exploration of agro-wastes and other renewable biomass wastes as a precursor of heterogeneous catalysts for transesterification has become more fascinating in contrast to the conventional homogeneous catalysts. This is mainly attributed by its peculiar characteristics such as easy separation, reusability, cost effectiveness, eco friendliness, etc. Hence, the potential of banana inflorescence (BI), a byproduct of banana cultivation with less economic value was investigated herein, for the development of a competent heterogeneous catalyst for profitable biodiesel production from Used cooking oil (UCO). The transformation in porosity, surface area and chemical composition of banana inflorescence, brought about by calcination was examined by Scanning electron microscopy (SEM), Brunauer–Emmett–Teller (BET), Powder X-ray diffractogram (XRD), Fourier transform infrared spectroscopy (FTIR) and Energy Dispersive X-ray Spectroscopy (EDS) analysis. The conversion was enumerated by Nuclear magnetic resonance (^{1}H NMR) spectroscopy and it was observed that transesterification using 2 wt% catalyst, 9:1 methanol to oil molar ratio for a reaction time of 75 min at 65 ºC showed a fatty acid methyl ester (FAME) conversion of 98.62%.

Keywords: *Banana inflorescence; Used cooking oil; Calcination; Biodiesel*

---

[a] *Department of Chemical Engineering, Erode Sengunthar Engineering College, Perundurai, Tamilnadu-638057, India*
[b] *Department of Mechanical Engineering, Government College of Technology, Coimbatore, Tamilnadu, India*
[c] *Department of Food Technology, Kongu Engineering College, Erode, Tamilnadu, India*
* *Corresponding author: vsanthoshchemical@gmail.com*

INTRODUCTION

Renewable energy resources are basic requisites for developing as well as developed nations and are the base for economic growth which in turn triggers the energy demand. Almost 80% of world's energy needs are met by fossil fuels, a primary energy source [1]. In today's world, where fuel prices are hiking due to spiraling demand and diminishing supply, the fuels are getting exploited in a rate faster than what nature can replenish. This is precisely evident from the statistics that points out the crude oil production of 36,468.97 ktoe (kilo tonne of oil equivalent) and import of 2,25,282.02 ktoe (kilo tonne of oil equivalent) by India in 2017-18 [2]. In India, 72% of transportation fuel is diesel, followed by 23% of petrol, 5% of CNG, LPG, etc. of which 80% of oil needs is dependent on imports [3]. Diesel plays a major role in transportation, agriculture, power generation, industries, mining, quarrying and private imports [2]. This precisely implicates a critical need for providing alternate energy sources in a sustainable manner, especially at a relatively affordable cost.

Besides the accelerated exploitation, the byproducts of the fossil fuel combustion has been imposing threat to health and climate mitigation. Concomitant with the growth of global energy consumption by 2.9 % in 2018, CO_2 emission grew up by 2% and share of non-fossil fuels has increased to 15.3%, a highest record in recent history [4]. Biodiesel is one such non fossil fuel that has a considerable heating value of 39–41 MJ/kg like fossil based gasoline (46 MJ/kg), petrodiesel (43 MJ/kg), petroleum (42 MJ/kg) and coal (32–37 MJ/kg). It is noteworthy that higher heating value (HHV) makes the fuel more economic and the fuel can be used without any modification in the diesel engine [5]. The physical properties of biodiesel are similar to that of fossil based diesel and are entirely dependent on the nature of feedstock. Furthermore, biodiesel emission is devoid of sulfur and aromatic compounds and has reduced emission of CO_2, CO, NO_X and other particulate matters [6]. Along with this, renewability, high flash point and biodegradability has made biodiesel as a promising fuel to either blend with diesel or as a complete substitute [7,8]. Hence, biodiesel has become an attractive alternate for mineral diesel in spite of the diminishing petroleum reserves and increasing environmental crisis.

Biodiesel is a mixture of mono alkyl esters of fatty acids that can be produced from various types of vegetable oils, animal fats, microbial oil, algal oil and waste oil by transesterification with methanol or ethanol using nucleophilic homogeneous or heterogeneous catalyst [9]. Biodiesel can be produced by various methods such as pyrolysis, micro-emulsion, dilution, microwave technology, reactive distillation, catalytic distillation, super fluid method and transesterification. But transesterification is preferred over other techniques due to its ease of operation, suitability for large scale production and fuel properties [10]. Selection of a feedstock is a key factor as it affects the cost, yield, physicochemical properties and purity of biodiesel and it should be easily procurable [11]. It has been reported that the physico-chemical properties vary with sources of collection which owes to the varying optimum conditions obtained for biodiesel production using similar catalyst [12]. UCO is of 2 types: first used cooking oil that is collected from restaurants and second used cooking which is generally dumped into landfills by street food sellers [13]. Hence the conversion of used cooking oil into biodiesel is environment friendly, economically feasible, sustainable and reduces the risk of disorders. Niju et al employed UCO as a feedstock for biodiesel production using different calcium based heterogeneous catalysts and reported a high biodiesel conversion [14-17].

Nowadays, heterogeneous catalysts seeks more attention due to easy catalyst separation and reusability [18]. Several agro-waste biomasses have been explored as precursor of catalyst for biodiesel production in the last few decades which includes *Musa balbisiana* trunk [19], *Musa balbisiana* underground stem [20] and *Musa balbisiana* peels [21]*, Musa paradisiacal* peels [22], *Musa acuminata* peels [23], *Musa acuminata* peduncle [24] and *Musa sp.* “Pisang Awak” peduncle [25], etc. India being the largest producer of banana (25.7 % globally) [26], generates a huge amount of banana inflorescence, that has quite low value due to its inconsistent demand, less shelf life and limited acceptance [27]. Banana inflorescence (botanical term-thryse) has a complex structure consisting of female flowers at proximal end followed by a male bud at the distal end which comprises of bracts enclosing male flowers [28]. While female flowers give rise to edible and economically valuable bananas, male buds are considered as waste during crop production with less economic value and are thrown away after harvesting leading to a huge post harvest waste, most of which are discarded in water bodies that increase the biological oxygen demand and affects the aquatic life [29]. Banana inflorescence can be used to treat dysentery, diabetes, ulcers, bronchitis, etc [30] and it is rich in polyphenols, dietary fibres and antioxidants [31]. Also, it is consumed as vegetable in many regions, particularly in India and Malaysia [29]. Eventhough it has tremendous nutritional and medicinal values, the tedious preparation process and less shelf life limits its consumption [32].

Hence the objective of the present work is to prepare a highly active heterogeneous catalyst from banana inflorescence (BI) and to test the catalytic activity for transesterification of UCO into biodiesel. The prepared catalyst was characterized using SEM, EDS, FTIR, XRD and BET techniques. Further, the biodiesel conversion was estimated by ^{1}H NMR analysis.

RESULTS AND DISCUSSION

Catalyst Characterization

Sem analysis

The surface morphology and particle size distribution of **CBIA (calcined banana inflorescence ash) and UBIP (uncalcined banana inflorescence peel)** was compared by means of Scanning electron microscopy (SEM) analysis and presented in Figure 1(a,b,c,d). UBIP (Figure 1(a,b)) has a rugged surface that is devoid of pores but has crevices whereas the CBIA (Figure 1(c,d)) has become relatively smoother and porous upon calcination.

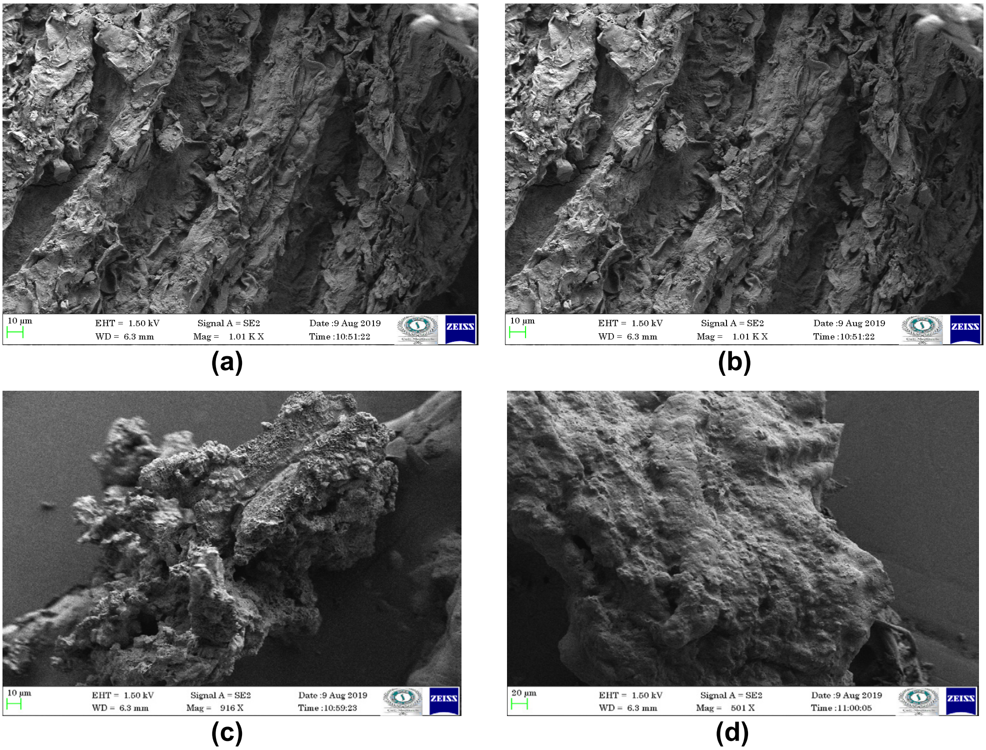

(a) (b)

(c) (d)

Figure 1. SEM images of UBIP (a and b) and CBIA (c and d)

The pores are formed due to the degradation of volatile organic compounds (VOCs) in the biomass to CO_2, CO, NO_2, etc [34]. Thus the calcination process increases the surface area in the form of porous structures for enhanced catalytic activity. This is evident through BET analysis which showed the increase in surface area from 0.879 m^2/g to 2.002 m^2/g. This is advantageous because a comparitively less amount of catalyst is sufficient which inturn increases the ratio of catalyst surface area to reactant volume, a crucial factor to increase collision rate and hence the reaction rate. Moreover the calcination process removes the undesired organic compounds in the form of gases leaving behind the minerals that are nonvolatile. Pathak et al (2018) reported similar observation of aggregates with mesopores and micropores after calcination of *Musa acuminata* peel for biodiesel production [22]. Balaji and Niju (2019) tested the potential of *Musa acuminata* peduncle as catalyst for biodiesel production wherein they reported the transformation of irregularly distorted particles into highly ordered pororus particles upon calcination [24].

BET analysis

In order to substantiate the increase in surface area upon calcination, BET analysis was performed with UBIP and CBIA. Before calcination, surface area was 0.877 m^2/g which increased to 2.002 m^2/g after calcination. As expected, there was more than two fold increase in the surface area upon calcination. Also, there was an increase in pore volume and diameter from 0.002 cc/g, 2.103 nm to 0.003 cc/g, 2.463 nm respectively. Pathak et al (2018) had performed similar studies with *Musa acuminata* peel and reported the increase in surface area to 1.4546 m^2/g upon calcination [23]. These findings illustrates the improvement of biomass surface area upon calcination which makes it effective as a catalyst in transesterification reaction.

FTIR analysis

FTIR spectroscopy is an analytical technique that identifies the organic, polymeric and in some cases inorganic compounds. It makes use of infrared rays (10,000 to 100 cm^{-1}) to irradiate the sample which absorbs a part and others get passed through i.e., transmitted. The absorbed radiation brings about rotational and/or vibrational energy to the sample molecules. Depending on the chemical structure, a unique spectral fingerprint is produced for each molecule [35]. Hence, in order to determine the changes in the chemical composition of banana inflorescent powder brought about by calcination, UBIP and CBIA were analysed by FTIR (Figure 2) and the corresponding functional groups were presented in Table 1. Before calcination, i.e., in UBIP, OH stretching is stronger due to the presence of moisture [21,23,25], C=O and C-H stretching is prominent, indicating the presence of aldehyde and ketones [36,37]. All these corresponding peaks are absent after calcination, i.e. in CBIA indicating its degradation. Instead the peaks C-O stretching of K_2CO_3 has become more prominent [21,25,32,50].

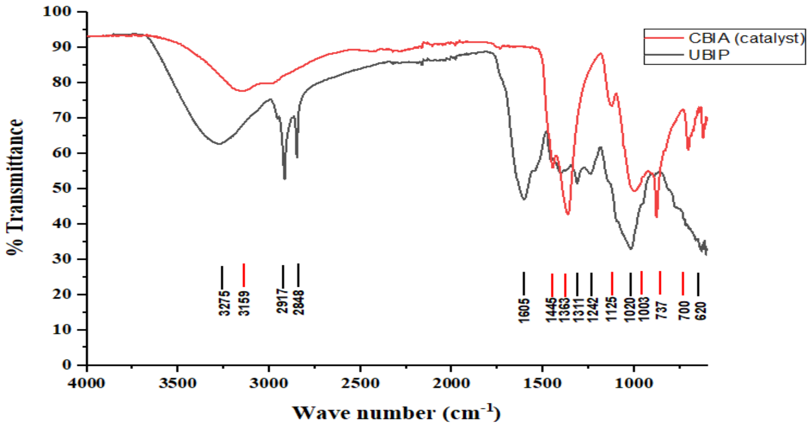

Figure 2. FTIR spectra of UBIP and CBIA

From the extent of transmittance, it is obscure that C=O stretching of K_2CO_3 has high absorbance which implies that potassium is present predominantly in the form of carbonates rather than oxides. OH stretching of $K_2CO_3.1.5\ H_2O$ denotes the association of small fraction of potassium carbonate with water molecules [25]. This may be due to the absorbance of CO_2 and moisture in atmosphere. Peaks for Si-O-Si stretching bands [33] and $CaCO_3$ was also observed but not as prominent as K [34]. These results are in concordance with the findings of Gohain et al (2017) [21], Pathak et al (2018) [23], and Balaji and Niju (2019, 2020) [24,25].

Table 1. Functional groups present in UBIP and CBIA detected from FTIR spectra

Wave number (cm^{-1})	CBIA	UBIP
700	CO_3^{-2} in metal carbonates	-
1003	Si-O-Si stretching bands	-
1020	-	C-O-C stretching at β(1→4)-glycosidic linkage of cellulose
1242	-	O-H Deformation
1311	-	C-N stretching of primary and secondary amines
1445	OH stretching in $K_2CO_3.1.5H_2O$	-
1605	K_2CO_3	C=O stretching
2848, 2917	-	Aliphatic C-H stretching
3159	K_2CO_3	-
3275	-	OH stretching NH in amine

EDS analysis

EDS is used for qualitative and quantitative analysis of chemical composition of any matter. It makes use of the unique atomic structure to differentiate the elements present in the sample that is irradiated with the beam of X-rays. The energy of emitted x-rays from the sample is a characteristic of the elements present in it [34]. The area of the peak indicates its abundance. Before calcination, only a fraction of metal ions are detected as most of them are bound to organic biomolecules [35]. After calcination, an obscure dominance of potassium was observed along with traces of Ca, Mg, Si, P, S, Cl, Br and Al. Calcination has enhanced the potassium content from 20.2 to 35.81 wt%, which is more than a two-fold increase. The detection of negligible amount of Br and S after calcination, is due to the removal of volatile organic compounds which in turn has increased its accessibility.

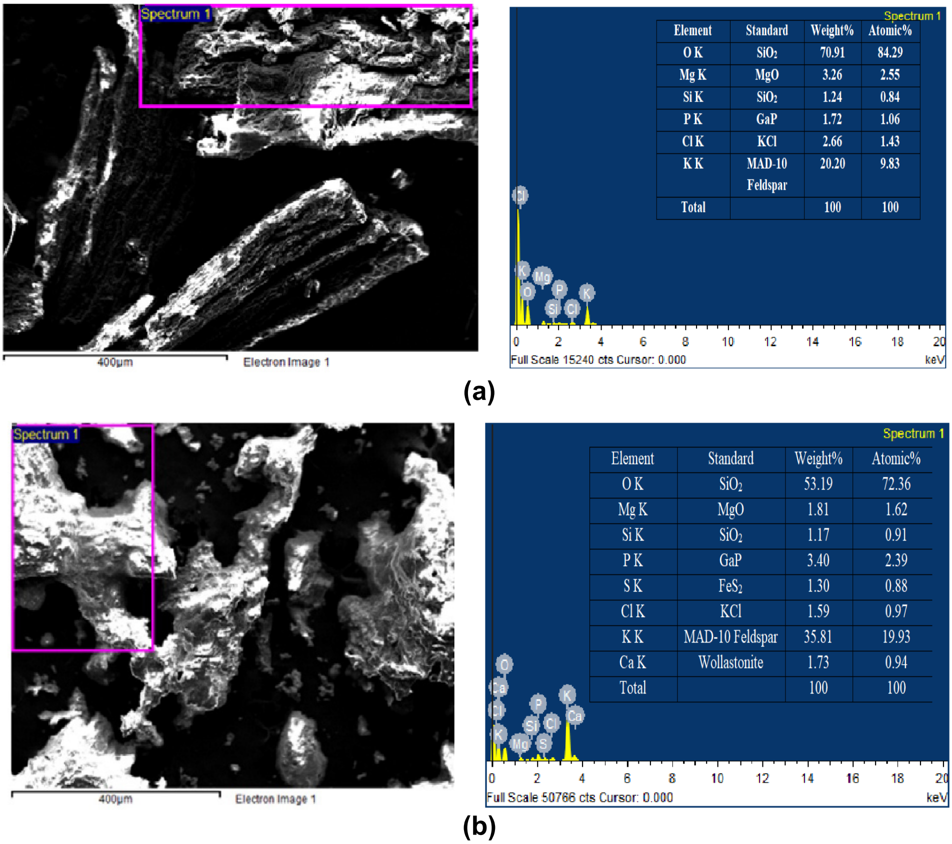

Element	Standard	Weight%	Atomic%
O K	SiO_2	70.91	84.29
Mg K	MgO	3.26	2.55
Si K	SiO_2	1.24	0.84
P K	GaP	1.72	1.06
Cl K	KCl	2.66	1.43
K K	MAD-10 Feldspar	20.20	9.83
Total		100	100

(a)

Element	Standard	Weight%	Atomic%
O K	SiO_2	53.19	72.36
Mg K	MgO	1.81	1.62
Si K	SiO_2	1.17	0.91
P K	GaP	3.40	2.39
S K	FeS_2	1.30	0.88
Cl K	KCl	1.59	0.97
K K	MAD-10 Feldspar	35.81	19.93
Ca K	Wollastonite	1.73	0.94
Total		100	100

(b)

Figure 3. Elemental composition of UBIP (a) and CBIA (b) from EDS analysis

This implies the significance of calcination process. The prevalence of oxygen and absence of carbon indicates the presence of minerals in the form of oxides rather than carbonates. Balaji and Niju (2019) examined *Musa acuminata* peduncle for biodiesel production wherein they reported an increase in K content from 25.63 wt% to 42.23 wt% upon calcination [24]. The previous works on agrowaste derived heterogeneous catalysts for transesterification were reported with abundance of K that contributed for its catalytic activity [20,21], [23,24].

XRD analysis

The presence of crystalline compounds in the UBIP and CBIA were detected by XRD analysis. In UBIP (Figure 4a), strong peaks corresponding to cellulose, a monoclinic crystal were observed between angles 2θ between 15.16° to 24.6°. Strong peaks corresponding to 2θ at 21.77°, 19.63° implies the presence of cellulose II whereas the peaks corresponding to 2θ at 15.16°, 14.54° implies the presence of cellulose II [36,37]. Cellulose I and Cellulose II are major plant cell wall components and the latter was detected predominantly in UBIP due to its thermodynamically stable crystalline nature [38]. After calcination i.e., in CBIA (Figure 4b), those peaks were absent indicating the combustion of cellulose and other volatile organic compounds (VOC) [34].

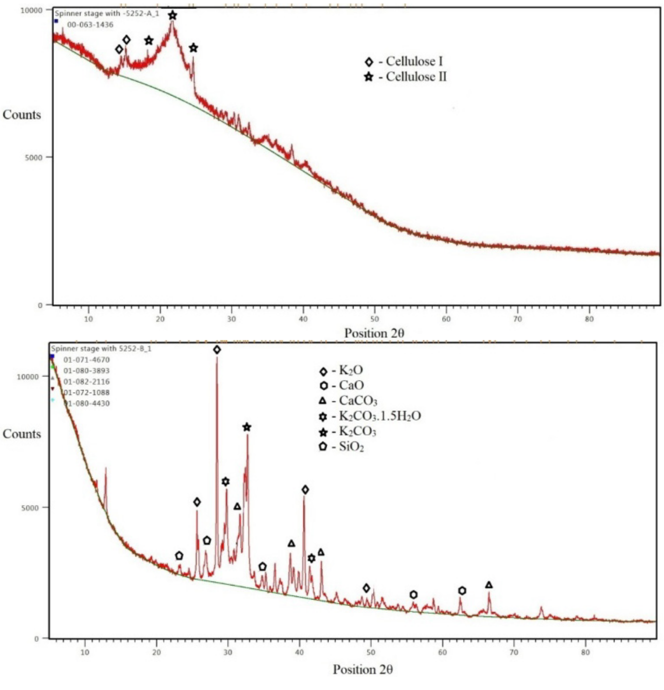

Figure 4. XRD spectra of UBIP (a) and CBIA (b)

Thus calcination reduces the background of organic compounds, allowing the trace minerals to be detected at high intensity. Strong characteristic peaks at angles 2θ of 25.66°, 25.86°, 40.62°, 41.4°, 28.45°, 33°, 30.5°, 42° were observed, indicating the predominance of K_2O, K_2CO_3 and $K_2CO_3.1.5H_2O$ [23,39]. Small peaks at angles 2θ of 30.85°, 39.19°, 43°, 67° indicates the presence of CaO and $CaCO_3$ [23,39]. Peaks corresponding to 24°, 28.5°, 34.5° indicates the presence of SiO_2 [23,39]. This clearly indicates the random distribution of several minerals in the form of oxides and carbonates. Moreover, Potassium was predominant among the minerals that is present in the CBIA. These results are in accordance with the findings of Gohain et al (2017) [21], Pathak et al (2018) [23], and Balaji and Niju (2019, 2020) [23,24].

Biodiesel characterization by ^{1}H-NMR analysis

Transesterification reaction was performed using 2 wt% CBIA catalyst with methanol to oil ratio of 9:1 at 65 ºC for a reaction time of 75 min. ^{1}H-NMR analysis was performed for quantitative estimation of FAME in the biodiesel. A characteristic peak of methyl group at 3.66 ppm that is prominent for a typical FAME is abundant, confirming the presence of biodiesel [35]. This is due to the substitution of glycerol part of glycerides with methoxy group. A triplet peak at 2.75-2.79 ppm indicates the presence of α-methylene group nearby to methoxy ester. Peak corresponding to 5.28-5.41 ppm denotes the presence of olefinic protons that is peculiar for unsaturated hydrocarbon chains. Peaks between 1.25-1.30 ppm represents the backbone CH_2 of the hydrocarbon chains.

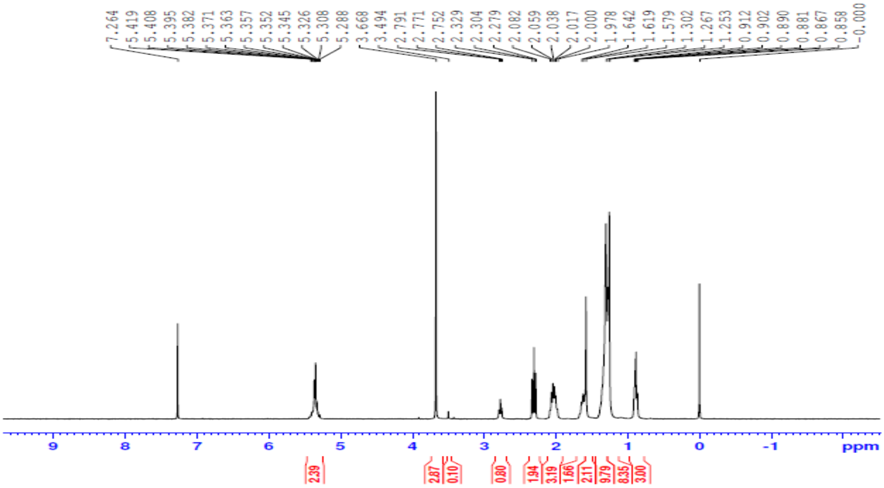

Figure 5. ^{1}H NMR spectrum of Biodiesel

Peaks between 0.85-0.91 ppm corresponds to the terminal methyl group. Presence of fatty acids were also detected by the peaks between 1.57-1.64 ppm [36,37]. Absence of peaks between 3.73 to 5.27 ppm denotes the absence of mono, di and triglycerides [38]. The percentage conversion of UCO to biodiesel was found to be 98.62 % using Eq.(1). This indicates the potential of CBIA as a catalyst for biodiesel production from UCO.

Comparison of different agro-residue based heterogeneous catalysts for biodiesel production

Potential of different biomass derived heterogeneous catalysts for biodiesel production was discussed. The catalytic activity of CBIA was compared with the state of the art in the literature and presented in Table 2. Deka and Basumatary (2011) investigated the transesterification of *Thevetia peruviana* oil using calcined *Musa balbisiana* trunk as a heterogeneous catalyst and reported 96% biodiesel conversion using 20 wt% catalyst, 10:1 methanol to oil ratio for a reaction time of 3 h [19]. Pathak et al (2018) made a similar study on transesterification of soybean oil with *Musa acuminata* peel at room temperature wherein they obtained 98.95% of biodiesel with 0.7 wt% catalyst, 6:1 methanol to oil ratio in 4 h [23]. Aslam et al (2014) examined the potential of *Musa balbisiana* underground stem for transesterification of *Jatropha curcas* into biodiesel but the high acidic value of the oil required transesterification at a high temperature (275 ºC) and pressure (4.2 Mpa) [20]. This shows the impact of physicochemical properties of the feedstock on FAME conversion. Betiku and Ajala (2014) reported a two step biodiesel synthesis from *Thevetia peruviana* oil to decrease the acid value by esterification and utilized *Musa paradisiacal* peel as a catalyst in transesterification process. The authors reported 95% yield of biodiesel by means of transesterification using 3 wt% catalyst, 3:0.9 methanol to oil ratio at 60 ºC for a reaction time of 75 min [22]. Balaji and Niju (2020) tested the catalytic activity of *Musa sp.* "Pisang Awak" peduncle for transesterification of esterified *Ceiba pentandra* oil into biodiesel wherein they reported an yield of 98.69±0.18% with 1.978 wt% catalyst loading, 9.20:1 methanol to oil ratio at 65 ºC for 60 min [25]. They have also reported the potential of *Musa acuminata* peduncle for transesterification of esterified *Ceiba pentandra* oil into biodiesel. However this process required 11.46:1 methanol to oil ratio with 2.68 wt% catalyst for 106 min at 65 ºC for a similar conversion of 98.73±0.5% [25]. Gohain et al (2017) had reported complete conversion of used cooking oil into biodiesel with 2 wt% calcined *Musa balbisiana pee*l, 6:1 methanol to oil ratio at 60 ºC. Eventhough used cooking oil does not require esterifcation this took a quite longer reaction time of 180 min [21]. In the present work, 98.62% of conversion of used cooking oil into biodiesel was achieved in 75 min with a single step transesterification using 2 wt% CBIA, 9:1 methanol to oil molar ratio at 65 ºC.

Table 2. Summary of potential of different agrowastes as precursor of catalyst for biodiesel production

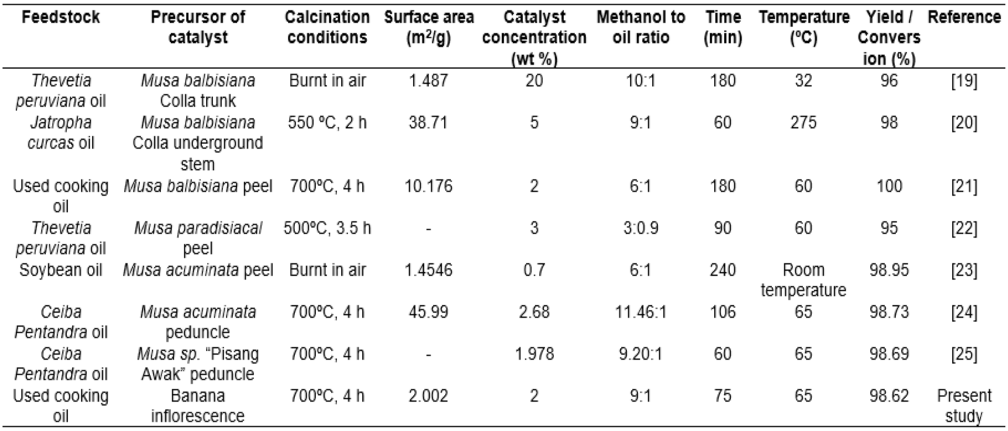

Feedstock	Precursor of catalyst	Calcination conditions	Surface area (m^2/g)	Catalyst concentration (wt %)	Methanol to oil ratio	Time (min)	Temperature (ºC)	Yield / Conversion (%)	Reference
Thevetia peruviana oil	*Musa balbisiana* Colla trunk	Burnt in air	1.487	20	10:1	180	32	96	[19]
Jatropha curcas oil	*Musa balbisiana* Colla underground stem	550 ºC, 2 h	38.71	5	9:1	60	275	98	[20]
Used cooking oil	*Musa balbisiana* peel	700ºC, 4 h	10.176	2	6:1	180	60	100	[21]
Thevetia peruviana oil	*Musa paradisiacal* peel	500ºC, 3.5 h	-	3	3:0.9	90	60	95	[22]
Soybean oil	*Musa acuminata* peel	Burnt in air	1.4546	0.7	6:1	240	Room temperature	98.95	[23]
Ceiba Pentandra oil	*Musa acuminata* peduncle	700ºC, 4 h	45.99	2.68	11.46:1	106	65	98.73	[24]
Ceiba Pentandra oil	*Musa sp.* "Pisang Awak" peduncle	700ºC, 4 h	-	1.978	9.20:1	60	65	98.69	[25]
Used cooking oil	Banana inflorescence	700ºC, 4 h	2.002	2	9:1	75	65	98.62	Present study

CONCLUSION

The present work elucidates the competency of CBIA in catalyzing the transesterification of used cooking oil into biodiesel. Morphological changes and improvement in the catalyst surface area from 0.877 mm^2/g to 2.002 mm^2/g upon calcination was evident from SEM and BET analyses. FTIR and XRD analyses confirmed the enrichment of potassium in the form of oxides and carbonates after calcination. EDS analysis unveiled a drastic increase of potassium from 20.20 to 36.22 wt% upon calcination. These data, altogether supports the theoretical basis of potential of banana inflorescence calcine as a heterogeneous catalyst. Thereby, an attempt was made to bringforth CBIA as a catalyst for an efficient biodiesel production. Further, transesterification with a catalyst loading of 2 wt % and methanol to oil ratio of 9:1, for a reaction time of 75 min at 65 ºC has yielded a FAME conversion of 98.62%.

EXPERIMENTAL SECTION

Materials and Chemicals

BI was collected from a Plantation field in Erode (Tamil Nadu, India). Analytical grade methanol (CH_3OH, 99.8%) was purchased from Hi Media Laboratories Pvt. Ltd., Mumbai. UCO was collected from a local restaurant near Erode (Tamil Nadu, India). It was filtered to remove the unwanted food particles and residues, followed by preheating at 105°C in hot air oven to remove the moisture content.

Catalyst Preparation

BI was washed with deionised water twice to remove the dust particles. In order to remove the moisture content, it was dried at 65 °C in hot air oven for 24 h. It was then made into a fine powder using a mixer grinder and sieved using ASTM 18 mesh size sieve (≤0.425 mm). The banana inflorescence powder (BIP) was calcined at 700 ºC separately for 4 h in muffle furnace to concentrate the minerals in the form of ash. Muffle furnace can be manually programmed for gradual increase, hold on and gradual decrease of temperature at a rate of 5 ºC/min to maintain the consistency and reliability. The calcined banana inflorescence ash (CBIA) catalyst was further stored in an air tight container.

Characterization of Catalyst

The surface morphology of uncalcined banana inflorescence peel (UBIP) and calcined banana inflorescence ash (CBIA) was explored by CARLZEISS SIGMA V model Scanning electron microscopy (SEM). The functional groups present in the UBIP and CBIA were detected by Fourier transform infrared spectroscopy (FTIR) using Thermo Scientific Ltd., spectrometer. X-ray diffraction (XRD) analysis was performed on both UBIP and CBIA to detect the crystalline components in the UBIP and CBIA using PANalytical X'Pert3 powder diffractometer.

The XRD Characterization was carried out using a Cu Kα radiation, 40 Kv and 30 Ma with over a 2θ range of 2 to 100° with a step size of 2° per minute. Energy dispersive X-ray spectroscopy (EDS) was performed to ascertain the elemental composition of both UBIP and CBIA. The Brunauer-Emmett-Teller (BET) analysis was performed by Quantachrome NovaWin (version 11.05) in order to identify the surface area, pore volume and pore diameter of both UBIP and CBIA.

Transesterification

The schematic representation of the workflow is presented in Figure 6. Transesterification of UCO with methanol using CBIA catalyst was performed in a 250 ml three neck round bottomed flask placed in the water bath which was set at 65 ºC. Middle neck was connected to a mechanical stirrer and one of the side necks was connected to a condenser and the other to temperature indicator. Transesterification reaction was performed at 65 ºC using 9:1 methanol to oil molar ratio, 2 wt% catalyst loading for a reaction time of 75 min. After the completion of reaction, the excess methanol was separated by rotary evaporator. The catalyst was then filtered by No.1 Whatman filter paper and the filtrate was transferred to a separating funnel. The phases were allowed to separate overnight. The top layer, biodiesel was separated and stored in a separate air tight container for further analysis. The bottom layer, glycerol which is a byproduct in transesterification process was collected and stored separately.

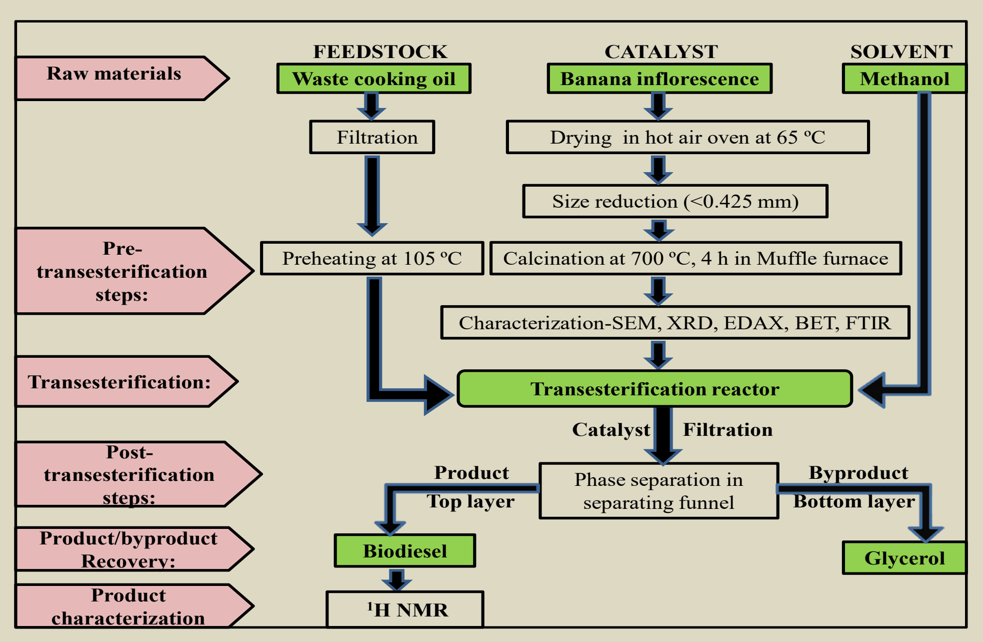

Figure 6. Schematic representation of workflow involved in biodiesel production

Biodiesel Characterization by NMR

The structural elucidation of fatty compounds present in the biodiesel was analysed by proton nuclear magnetic resonance (^{1}H NMR) using Bruker biospin. This aids in the quantitative determination of fatty acid methyl esters in the biodiesel in terms of % conversion.

The % conversion was calculated by the following formula (Eq.1) [33],

$$\% \text{ Conversion} = \frac{2\text{A}_{\text{ME}}}{3\text{A}_{\alpha-\text{CH}_2}} \times 100 \quad (1)$$

where,

% conversion = % FAME in Biodiesel,
A_{ME} = Area of peak at 3.7 ppm corresponding to methyl group of FAME,
$A_{\alpha-\text{CH}_2}$ = Area of peak corresponding to 2.3 ppm α-methylene group of FAME.

ACKNOWLEDGEMENTS

There are no acknowledgements.

REFERENCES

1 D. Huang; H. Zhou; L. Lin; *Energ Procedia.,* **2012**, *16*, 1874-1875.
2 G.S. Lakshmi; S. Bhawna; K. Amit; S.V.K. Shobha; *Energy statistics,* **2019.**
3 M.R. Nouni; P. Jha; R. Sarkhel; C. Banerjee; A.K.Tripathi; *J. Manna Fuel;* **2021**, *305*, 121583.
4 U.K. Pata; A.Kumar; *Water*; **2021,** *13(10)*, 1387.
5 A. Demirbas; *Energ. Policy,* **2007***, 35,* 4661-4670
6 S. Basumatary; B. Nath; P. Kalita; *J. Renew. Sust. Energ.,* **2018***, 10,* 043105.
7 P.A. Handayani; A. Abdullah; H. Hadiyanto; *Period. Polytech. Chem. Engi.,* **2019**, *63*, 406-413.
8 W. Shi; J.Li; B. He; F. Yan; Z. Cui; K. Wu; L. Lin; X. Qian; Y. Cheng; *Biores. Tech.*, **2013**, *139*, 316-322.
9 M. Kaur; A. Ali; *Renew. Ener.,* **2011**, *36*, 2866-2871.
10 E. Bet-Moushoul; K. Farhadi; Y. Mansourpanah; A.M. Nikbakht; R. Molaei; M. Forough; *Fuel., **2016**, 164*, 119-127.
11 A. Demirbas; *Biomass and Bioenerg.,* **2009**, *33*, 113-118.
12 A.N. Phan; T.M. Phan; *Fuel.,* **2008**, *87*, 3490-3496.
13 W. Asri; A. Budiman; *Phy. Procedia,* **2013,** *32*, 190-199.
14 S.Niju; K.M.M Sheriffa Begum; N. Anantharaman; *Env. Prog. Sust. Ener.*, **2015**,

34, 248-254.
15 S.Niju; K.M.S Begum; N.Anantharaman; *Int. J. Green Energ.,* **2016**, *13*, 1314-1319.
16 S. Niju; R. Rabia; K.S Devi; M.N. Kumar; M. Balaji; *Waste and Biomass Valorization,* **2018**, *11*, 793-806. https://doi.org/10.1007/s12649-018-0520-6
17 S. Niju; M. Kirthikaa; S. Arrthi; P. Dharani; S. Ramya; M. Balaji; *J. Inst. Eng. India,* **2019***, 101*, 53-60.
18 I. Ambat; V. Srivastava; M. Sillanpa; *Renew. Sust. Ener. Rev.,* **2018**, *90*, 356-369.
19 D.C. Deka; S. Basumatary; *Biomas and Bioener.,* **2011**, *35*, 1797-1803.
20 A. Kumar; S. Prashant; *Cat let.*, **2014**, *144*, 1344-1353.
21 M. Gohain; A. Devi; D. Deka; *Ind. Cro. Prod.,* **2017**, *109*, 8-18.
22 E. Betiku; S.O. Ajala; *Ind. Cro. Prod.,* **2014**, *53*, 314-322.
23 G. Pathak; D. Das; K. Rajkumari; L. Rokhum; *Green Chem.*, **2018**, *20*, 2365-2373.
24 M. Balaji; S. Niju; *Ene. Conv. Manag.,* **2019**, *189*, 118-131.
25 M. Balaji; S. Niju; *Ren. Ener.,* **2020**, *146*, 2255-2269.
26 P.R. Sudha; Vidyadhar; S. Mamta; R. Rajesh; K. Pankaj; B. Hemanga; T. Bhawna; Ministry of Agriculture and Farmers' Welfare, New Delhi, India.
27 B.S. Padam; H.S. Tin; F.Y. Chye; M.I. Abdullah; *J. Food. Sci. Tech.,* **2014**, *51*, 3527-3545.
28 B.F.Lau; K.W. Kong; K.H. Leong; J. Sun; X. He; Z. Wang; M.R. Mustafa; T.C. Ling; A. Ismail; *Trends in Food Science and Technology*, **2020**, *97,* 14-28.
29 P.F. Zehla; D. Vijayalakshmi; V.C. Suvarna; S.Yatnatti; *Int. J. Curr. Micro. and App. Sci.*, **2018**, *7*,1243-1250.
30 K.S. Kumar; D. Bhowmik; S. Duraivel; M. Umadevi; *J. Pharm and Phytochem.*, **2012**, *1*, 51-63.
31 J.J Bhaskar; N.D. Chikunda; P.V.Salimath; *J. Agri. and Food Chem.*, **2011**, *60(1)*, 427-432.
32 A. Krishnan; V.R. Sinija; *Int. J. Agri. and Food Sci Tech.,* **2016***, 7*, 13-22.
33 G. Gelbard; O. Bres; R.M. Vargas; F. Vielfaure; U.E. Schuchard; *J. Amer. Oil Chem. Soc.*, **1995**, *72*, 1239-1245.
34 L. Gustavsson; M.L. Karlsson; *Adv. in Therm. Bio. Conv.*, **1993**, 1522-1532.
35 R.M. Silverstein; X.F. Webster; J.D. Kieml; John Wiley & Sons., Inc., USA, **2005**.
36 Y. Inbar; Y. Chen; Y. Hadar; *Soil Sci.*, **1991**, *152*, 272-282.
37 I.M. Mendonca; Paes, A.R.L. Orlando; Maia; J.S. Paulo; M.P. Souza; C. Silva; *Renew. Ene.*, **2019**, *130*, 103-110.
38 F.A. Miller; C.H. Wilkins; *Anal. Chem.*, **1952**, *24(8)*, 1253-1294.
39 E. Betiku; A.M. Akintunde; T.V. Ojum; *Energy,* **2016**, *103*, 797-806.
40 D. Shindo; T. Oikawa; *Anal. Elec. Micro. for Mat. Sci.*, **2002**, 81-102.
41 D. Fancello; J. Scalco; D. Medas; E. Rodeghero; A. Martucci; C. Meneghini; G.D.Giudici; *Int. J. Env. Pub. Hea.,* **2019**, *16(11)*, https://doi.org/10.3390/ijerph16111976
42 A.D. Frenc; *Cellulose,* **2014**, *21*, 885-896.

43 J. Gong; J. Li; J. Xu; *RSC Advances,* **2017**, *7*, 33486-33493.
44 S. Kumar; R. Gupta; Y.Y. Lee; R.B. Gupta; *Biores. Tech.*, **2010**, *101*, 1337-1347.
45 M. Sharm; A. Ali; S.K. Puri; D.K. Tuli; *Biomass and Bioenerg.*, **2012**, *41*, 94-106.
46 V.M. Mello; F.C.C. Oliveira; W.G. Fraga; J.S. Claudia; A.Z. Paulo; *Mag. Res. Chem.,* **2008**, *46*, 1051-1054.
47 F. Faraguna; M. Racar; Z. Glasovac; A. Jukic; *Energ. and Fuels,* **2017**, *31*, 3943-3948.
48 J.K. Satyarthi; D. Srinivas; P. Ratnasamy; *Energ. and Fuels,* **2009,** *23*, 2273-2277.
49 B. Nieva-Echevarría; E. Goicoechea; M.J.G Manzanos; *Food Res. Int.,* **2014**, *66*, 379-387.
50 Y. Zhou; M. Chen; X. Dong; D. Yang; *Molecules,* **2024**, 29(17), https://doi.org/10.3390/molecules29174113